Fullerides

DOI: 10.1002/anie.201105360

Direct Observation of the Transition from Static to Dynamic Jahn–Teller Effects in the $[Cs(THF)_4]C_{60}$ Fulleride**

*Konstantin Yu. Amsharov, Yvonne Krämer, and Martin Jansen**

Fullerenes feature a number of unique chemical and physical phenomena. Among these the commonly high electron affinity allows for an easy uptake of excess electrons.[1] In most cases, the resulting anions are open-shell species, which give rise to a variety of fascinating electronic effects in fulleride-based extended solids, such as superconductivity or ferromagnetism.[2,3] The mechanisms behind these collective properties are not yet fully clarified, however, they have been tentatively associated to respective local electronic structures.[1] For C_{60}, and also for many other highly symmetric fullerene cages, the frontier orbitals are degenerate and may get unequally occupied upon reduction. Such a scenario inevitably should result in a Jahn–Teller effect (JT).[1,4] Meanwhile, a number of theoretical analyses have become available, which all agree in that the JT distortion should be fairly small, leading to orbital splittings of less than 0.1 eV.[5] As a geometric response, most investigators have considered a global distortion of the C_{60} cage to an ellipsoidal body.

Single-crystal X-ray structure determination is the most definitive experimental technique for detailed structural analyses and investigation on JT distortions of fullerides in the solid state. Unfortunately the progress in this field has been impaired by the difficulty in synthesis of high-quality single crystals. Fulleride crystals are frequently twinned and suffer from orientational disorder of the spherelike C_{60} anions. Although, in few cases reliable crystal data have been obtained,[6–8] the experimental evidence for a JT effect in anionic C_{60} has remained ambiguous, at least inconsistent. Even when considering only structure determinations of high accuracy, the results for C_{60}^{2-} vary from virtually spherical to significantly elongated shapes[7b,d] Thus, intriguingly the issue of a static JT distortion in C_{60}^{2-} is far from being settled. Quite understandable, the situation is even worse for the monoanion $C_{60}^{-\bullet}$, where the effects are expected to be even more subtle. The reasons behind this dissatisfactory situation are the faintness of the orbital splittings and geometric distortions expected, and lack of precise crystal structure determinations.

Here we report on $[Cs(THF)_4]C_{60}$, the synthesis and growth of fully ordered single crystals, which have been used to monitor for $C_{60}^{-\bullet}$ the structural and electronic implications of the JT theorem, in particular to directly observe the transition from static to dynamic JT effects.

The C_{60} anion radicals were obtained from solid C_{60} in a THF/octane mixture by reduction with metallic Zn in the presence of CsOH.[9] The fulleride crystals were grown in sealed all-glass systems by gradient solvent exchange as described elsewhere.[6a] $[Cs(THF)_4]C_{60}$ crystallizes as black block-shaped crystals of up to 10 mm in diameter. The compound was found to be unexpectedly stable, particularly no decomposition (as confirmed by repetitive X-ray analysis) was noticeable after exposure to air for several weeks. Nevertheless, as a precaution, all sample preparations and manipulations were carried out under anaerobic conditions.

The crystal structure has been determined from single-crystal data and refined on data sets recorded at 200, 175, 150, 125, 100, and 50 K. The following description of the structure is based on the 50 K data.[10]

The anionic and cationic building units, respectively, are the radical anion $C_{60}^{-\bullet}$ and cationic $[Cs(THF)_4]^+$, where four THF molecules act as monodentate ligands forming a square-planar complex. No free solvent molecules are present in the structure. The coordination sphere of cesium is completed by two fullerene anions forming a sandwich $[Cs(THF)_4(\eta^6\text{-}C_{60})_{2/2}]$ (Figure 1). Each fullerene anion is twofold coordinated by Cs, resulting in a linear chain of alternating cations and anions (Figure 2). The packing of the respective chains gives a square 2D fullerene net, where each $C_{60}^{-\bullet}$ has four fullerene neighbors with short center-to-center intralayer distances of about 9.94 Å, whereas the shortest interlayer separation is substantially larger and amounts to 13.09 Å. Two of the coordinated THF molecules partially protrude into voids of the interfullerenes, preventing the anion radicals from dimerization.[11] Such an atypical square-shaped organization of fullerene anion radicals with short interfullerene contacts have been regarded sufficient to manifest 2D metallic behavior.[6b]

A closer inspection of the bond lengths in $C_{60}^{-\bullet}$ reveals a significant degree of deviation from the ideal I_h symmetry, indicating some systematic symmetry reduction as required in terms of the JT theorem. Relative to neutral C_{60}, the average length of the 6:6 bonds is increased from 1.383 Å to 1.396(1) Å whereas the average of the 5:6 bond lengths is reduced from 1.453 Å to 1.449(1) Å.[13] These changes are consistent with the now partially occupied t_{1u} LUMO of C_{60} which is antibonding with respect to the 6:6 bonds and bonding with respect to the 5:6 bonds.[5,14] The changes found are slightly less pronounced than in the case of the C_{60}^{2-} dianion.[7]

The minimal symmetry reduction paths for lifting the degeneracy of the originally triply degenerate HOMO of $C_{60}^{-\bullet}$

[*] Dr. K. Y. Amsharov, Dipl. Chem. Y. Krämer, Prof. Dr. M. Jansen
Max Planck Institute for Solid State Research
Heisenbergstraße 1, 70569 Stuttgart, Germany

[**] The authors are grateful to Dr. Jürgen Nuss for collecting X-ray data, Dr. Reinhard Kremer for EPR measurements, Ms. Eva Brücher for SQUID measurements, Mr. Nils Schumacher for assistance with synthesis, and Dr. Pavel Kazin for helpful discussions.

Supporting information for this article is available on the WWW under http://dx.doi.org/10.1002/anie.201105360.

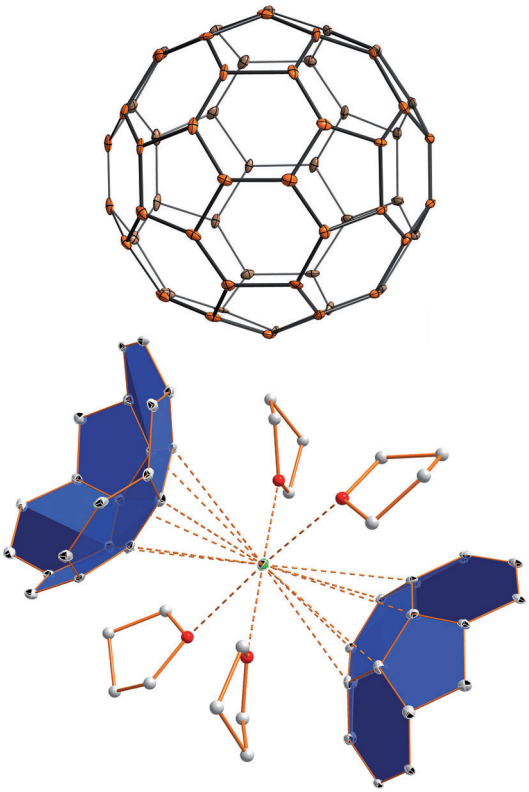

Figure 1. Top) ORTEP plot of the C_{60} anion radical in $[Cs(THF)_4]C_{60}$ at 50 K. Displacement ellipsoids are drawn at 50% probability level. Bottom) Sandwichlike $[Cs(THF)_4(\eta^6\text{-}C_{60})_{2/2}]$ fragment showing Cs^+ coordinated by four THF and two $C_{60}^{-\bullet}$ molecules. Hydrogen atoms are omitted for clarity. Only sumanene fragments of C_{60} are displayed.

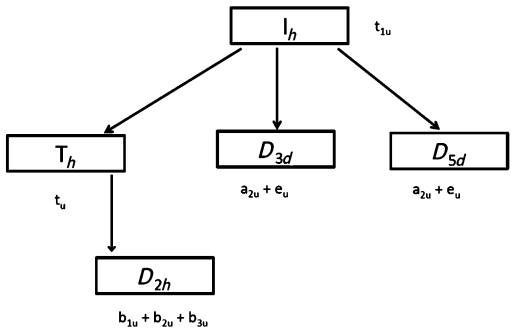

Scheme 1. The minimal symmetry reduction paths for lifting the degeneracy of the originally triply degenerate HOMO (t_{1u}) of $C_{60}^{-\bullet}$ by a JT distortion.

by a JT distortion are displayed in Scheme 1. Indeed, the deviations of the 6:6 carbon–carbon bond lengths as compared to unperturbed C_{60} are systematic, which is fortunately not biased by the crystallographic site symmetry of $C_{60}^{-\bullet}$ (C_1). On the other hand, because of the interactions with counter ions and a low-symmetry environment, the $C_{60}^{-\bullet}$ is probably not fully in its intrinsic geometry. The possible point group symmetries (see Scheme 1) would split the ensemble of 6:6 bonds into subsets, which we tested for consistency after averaging. This procedure needs to be repeated for all possible choices for the unique five-, three-, and two-fold

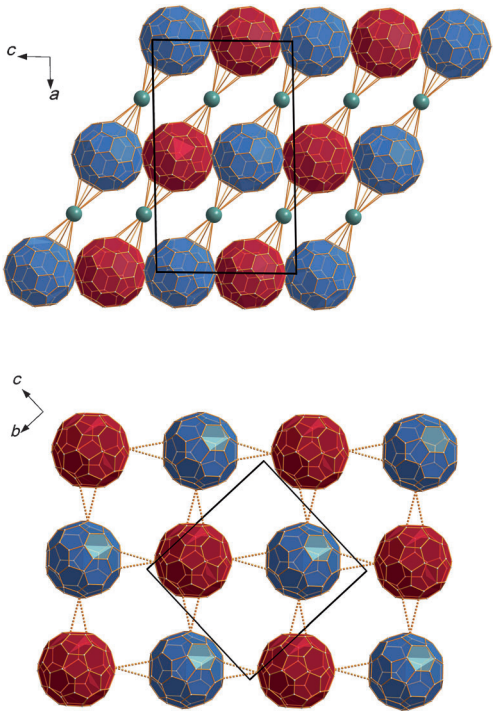

Figure 2. Top) Projection of the crystal structure along the [010] direction showing C_{60}–Cs individual chains (coded by blue and red colors) and layers of $C_{60}^{-\bullet}$. The unit cell is shown in black. THF molecules are omitted for clarity. Bottom) A C_{60} layer with square-shaped arrangement of the fullerene molecules. The short intermolecular C···C contacts of less than 3.3 Å are marked by dashed lines.

axes with respect to pristine C_{60}. The experimentally found variations comply best with the point group D_{3d}, and that only for one out of the possible ten C_3 rotation axes of C_{60} (see Figure 3). Three out of six possible orientations for the unique axes of point group D_{5d} also show patterns of selective bond elongations. This is, however, mainly effected by the D_{3d} symmetry which exactly relates these three orientations of the five-fold axes. Out of the 15 orientations of two-fold rotation axes only one sticks out, approximately fulfilling D_{2h} point group symmetry. These observations are in accordance with locally distorted $C_{60}^{-\bullet}$ species, basically of point symmetry D_{3d} and D_{2h}, which appear superimposed in the crystal because of the spatial/temporal averaging of X-ray diffraction studies. The local elongation of specific 6:6 bonds at the same time produces a global deformation of the C_{60} sphere, with the asphericity growing with decreasing temperature. Global and local distortions appear to be correlated because the direction of global elongation of the cage coincides with the orientation of the unique axes. This finding is suited to settle the dispute on global and/or local distortions, since selective changes of bond lengths which are in accordance with a lower symmetric point group also would inevitably affect the overall shape of the cage.

The rather precise structural information as obtained from 50 K diffraction data clearly gives evidence for a static JT distortion. The picture obtained appears somewhat obscured because of the unresolved superposition of two different distortion patterns. Coexistence of more than one symmetry-reduced species as well as disorder in the crystal is

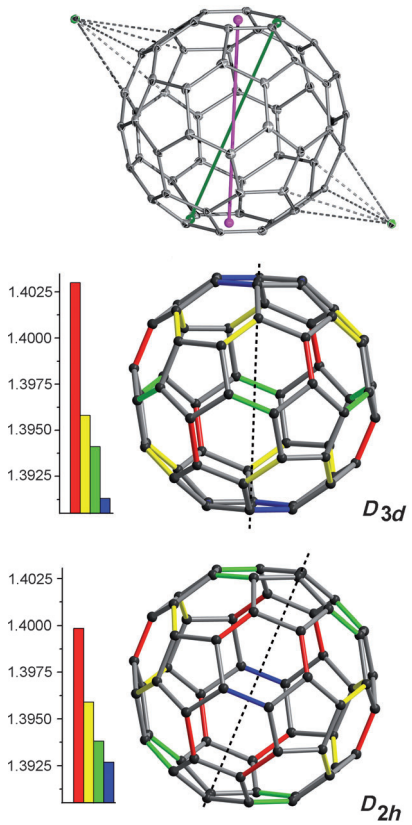

Figure 3. Positions of the symmetry inequivalent (6,6)-bonds in the C_{60} anion for the D_{3d} and D_{2h} representation. The four different types are shown by different colors. The color code of the predicted decreasing trend of the bond length is: red > yellow > green > blue.[7a] The bars show experimentally derived averages of the D_{3d} and D_{2h} subsets of corresponding C–C bond lengths. The respective three- and two-fold axes are given by dashed lines.

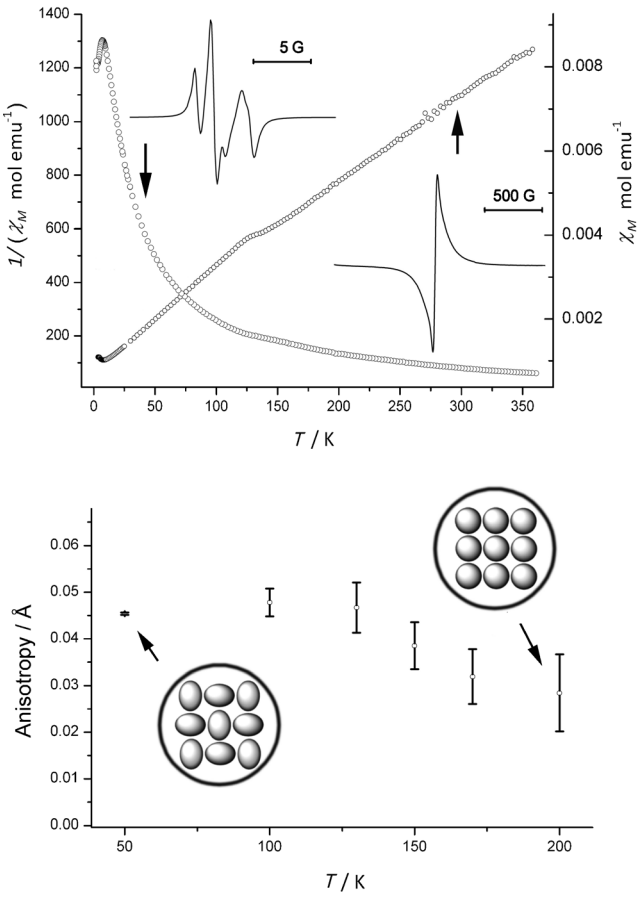

Figure 4. Observation of the transition from static to dynamic Jahn–Teller effects in $[Cs(THF)_4]C_{60}$. Top) Temperature dependence of the molar magnetic susceptibility (χ_M) and inverse molar magnetic susceptibility ($1/\chi_M$) of $[Cs(THF)_4]C_{60}$. The insets show the EPR lines of the LT and HT phases. Bottom) The temperature dependence of the global anisotropy of $C_{60}^{-\bullet}$ cage. The circlar insets show schematically the relative direction of elongation in the fullerene cages within the square fullerene layer.

well understandable: the energy differences between the configurations discussed is very small. To corroborate the structural findings temperature-dependent magnetic susceptibility and EPR measurements were performed.

Magnetic measurements were performed in the 2–360 K range. As it can be seen from the temperature dependence of the inverse molar magnetic susceptibility ($1/\chi_M$) the title compound undergoes a phase transition at about 150 K (Figure 4). Over the ranges 15–90 K and 160–360 K, the molar magnetic susceptibility can be fitted by the Curie–Weiss law $\chi_M = C/(T-\theta) + \chi_0$ with a constant $\chi_0 = 4.5 \times 10^{-4}$ emu mol^{-1}. The θ value was found to be -17 K for the low-temperature region (LT), and -23 K for the high-temperature region (HT). The C value of 0.27 emu K mol^{-1}, which is virtually the same for the LT (0.268) and HT (0.271) converts to an effective magnetic moment of 1.47 μ_B per formula unit. This corresponds to a contribution of about 72% of the spins from the total amount of C_{60} present. Similarly low C values were observed previously in 2D fulleride-based metal-containing close-packed $C_{60}^{-\bullet}$ layers and were attributed to antiferromagnetic interactions.[6b] However, such an explanation would not apply in the present case, because this effect has been appropriately accounted for by the Curie–Weiss law. Since the corresponding phase transition takes place in a rather wide temperature interval (110 K-170 K) the EPR spectra of the LT and HT phases were recorded at 50 and 300 K, far off the transition temperature (Figure 4). The EPR spectrum of the HT phase shows a broad isotropic signal with a peak-to-peak line width of about 150 G ($g = 2.0002$) which decreases dramatically to approximately 6 G for the LT phase (75 K) and develops a remarkable anisotropy. Such a behavior has been addressed before for $C_{60}^{-\bullet}$ and has been tentatively associated to a transition from static to dynamic JT effects.[1,15] The anisotropy of the LT phase spectrum gives evidence for a static $C_{60}^{-\bullet}$ distortion from I_h symmetry whereas for the HT phase the effect appears to become dynamic on the EPR time scale and an isotropic signal is observed: due to dynamic averaging of the distorted JT structures the anisotropy collapses and gives effective icosahedral symmetry (pseudorotation).

The structural transformations in the system were analyzed in the phase transition region by X-ray crystallography at 200, 175, 150, 125, 100, and 50 K. Neither irregular changes in the lattice parameters, nor in the relative position and orientation of individual molecules have been observed.

However, a detailed analysis reveals that the fullerene molecules undergo a significant deformation and finally assume an ellipsoidal shape at low temperature. For an evaluation of the degree of ellipsoidal deviation from the ideal sphere we have considered the anisotropy effect as a difference between longest and shortest carbon-to-carbon diameters. The results of anisotropy changes are visualized in Figure 4, showing the transition at the same temperature interval found by magnetic measurements. The anisotropy factor of about 0.0030 Å found for the HT phase is close to the anisotropy factor observed for pristine C_{60}[13] and might be related to crystal packing effects. Decreasing the temperature causes an increase in the anisotropy within the interval of 130–160 K to approximately 0.048 Å. This value stays constant during further cooling. The anisotropy value of 0.048 Å is between the values experimentally found for pristine C_{60} (0.02 Å) and the C_{60} dianion (0.07 Å), which is in good agreement with prediction.[1]

In summary, the facile synthesis and structural analysis of a highly ordered Cs-based fulleride are reported. The data obtained provide structural information sufficient to prove a JT distortion in the C_{60} anion radical. Also, for the first time the transition from static to dynamic Jahn–Teller effects in fullerides has been observed directly by X-ray analysis. The comprehensive structural information available, the presence of an extended fullerene network with short interfullerene contacts and antiferromagnetic ordering at $T_N = 7$ K offers promising opportunities for in-depth examinations of collective magnetic and transport phenomena in fullerides.

Experimental Section

Synthesis of $[Cs(THF)_4]C_{60}$: Fullerene C_{60} (50 mg, 0.0069 mmol, "MER Corporation", USA, 99,9%) have been reacted with zinc powder (4 mg, 0.0061 mmol) and cesium hydroxide (10 mg) in tetrahydrofuran (9 mL) containing *n*-octane (1 mL) and water (0.2 mL). The reaction mixture was cooled with liquid nitrogen and degassed under vacuum (2×10^{-3} mbar). The reaction was allowed to warm to room temperature and was stirred for 10–20 h resulting in a dark red-purple solution. Crystal growth was achieved by gradient solvent exchange as described elsewhere.[6a] All manipulations were carried out in all-glass system excluding any contamination.

Structure determination: For X-ray diffraction experiments a black platelike crystal was selected from the sealed off ampoule, transferred to a high-viscous oil and was attached to a loop. The intensity data of the single crystal were collected with a Smart APEX II diffractometer (Bruker AXS, Karlsruhe, Germany) with Mo-*K*a radiation (0.071073 Å) at different temperatures. Data reduction was carried out with the Bruker Suite software package, absorption correction was applied using SADABS. The structure was solved by direct methods and refined by full-matrix least-square fitting with the SHELXTL software package. We did not use constrains and restrains during the structure refinement.

The magnetic susceptibility, $\chi(T)$, was recorded on a Quantum Design "MPMS XL" magnetometer at magnetic fields of 0.1, 1, and 7 T in a temperature range of 2–370 K.

Received: July 29, 2011
Published online: October 11, 2011

Keywords: fullerenes · Jahn–Teller effect · radical ions · X-ray diffraction

[1] C. A. Reed, R. D. Bolskar, *Chem. Rev.* **2000**, *100*, 1075–1120, and references therein.
[2] a) A. F. Hebard, M. J. Rosseinsky, R. C. Haddon, D. W. Murphy, S. H. Glarum, T. T. M. Palstra, A. P. Ramirez, A. R. Kortan, *Nature* **1991**, *350*, 600; b) M. J. Rosseinsky, *Chem. Mater.* **1998**, *10*, 2665–2685.
[3] a) P. M. Allemand, K. C. Khemani, A. Koch, F. Wudl, K. Holczer, S. Donovan, G. Grüner J. D. Thompson, *Science* **1991**, *253*, 301–302; b) P. W. Stephens, D. Cox, J. W. Lauther, L. Mihaly, J. B. Wiley, P. M. Allemand, A. Hirsch, K. Holczer, Q. Li, J. D. Thompson, F. Wudl, *Nature* **1992**, *355*, 331–332.
[4] a) H. A. Jahn, E. Teller, *Proc. R. Soc. London Ser. A* **1937**, *161*, 220–235; b) N. Manini, E. Tosatti, *Jahn–Teller and Coulomb correlations in fullerene ions and compounds*, Lambert Acadmic Publishing, Saarbrücken, **2010**; c) O. Gunnarsson, *Alkali-doped fullerides: narrow-band solids with unusual properties*, World Scientific, Singapore, **2004**.
[5] W. H. Green, Jr., S. M. Gorum, G. Fitzgerald, P. W. Fowler, A. Ceuleman, B. C. Titeca, *J. Phys. Chem.* **1996**, *100*, 14892–14898.
[6] a) N. V. Kozhemyakina, J. Nuss, M. Jansen, *Z. Anorg. Allg. Chem.* **2009**, *635*, 1355–1361; b) D. V. Konarev, S. S. Khasanov, A. Otsuka, M. Maesato, G. Saito, R. L. Lyubovskaya, *Angew. Chem.* **2010**, *122*, 4939–4942; *Angew. Chem. Int. Ed.* **2010**, *49*, 4829–4832; c) W. Chou Wan, X. Liu, G. M. Sweeney, W. E. Broderick, *J. Am. Chem. Soc.* **1995**, *117*, 9580–9581; d) D. V. Konarev, A. V. Kuzmin, S. V. Simonov, S. S. Khasanov, E. I. Yudanova, R. N. Lyubovskaya, *Dalton Trans.* **2011**, *40*, 4453–4458.
[7] a) N. V. Kozhemyakina, J. Nuss, M. Jansen, *Eur. J. Inorg. Chem.* **2009**, 3900–3903; b) K. Himmel, M. Jansen, *Inorg. Chem.* **1998**, *37*, 3437–3439; c) K. Himmel, M. Jansen, *Eur. J. Inorg. Chem.* **1998**, 1183–1186; d) P. Paul, Z. W. Xie, R. Bau, P. D. W. Boyd, C. A. Reed, *J. Am. Chem. Soc.* **1994**, *116*, 4145–4146.
[8] M. B. Boeddinghaus, M. Salzinger, T. F. Fässler, *Chem. Eur. J.* **2009**, *15*, 3261–3267.
[9] M. Wu, X. Wei, L. Qi, Z. Xu, *Tetrahedron Lett.* **1996**, *37*, 7409–7412.
[10] Crystal Data: monoclinic; space group *Cc*; $a = 22.7337(1)$ Å, $b = 14.4469(7)$ Å, $c = 13.6650(6)$ Å; $V = 4486.1$ Å^3, $Z = 4$; $2\theta_{max} = 74.9°$; $-38 < h < 38$, $-24 < k < 24$, $-23 < l < 23$; $\lambda = 0.71073$ Å; $T = 50(2)$ K; final R value 0.0276 ($R_w = 0.0704$). CCDC 837149 (50 K), 837150 (170 K) contain the supplementary crystallographic data for this paper. These data can be obtained free of charge from The Cambridge Crystallographic Data Centre via www.ccdc.cam.ac.uk/data_request/cif.
[11] When the anion radicals $C_{60}^{-\bullet}$ are allowed to approach each other, they normally recombine and form diamagnetic single bonds $(C_{60})_2^{2-}$.[12] To the best of our knowledge, only four structures have been reported in which individual C_{60} anion radicals remained separated at low temperatures.[6]
[12] a) N. Kozhemyakina, K. Yu. Amsharov, J. Nuss, M. Jansen, *Chem. Eur. J.* **2010**, *16*, 1798–1805; b) D. V. Konarev, S. S. Khasanov, G. Saito, A. Otsuka, R. N. Lyubovskaya, *J. Mater. Chem.* **2007**, *17*, 4171–4177; c) D. V. Konarev, S. S. Khasanov, G. Saito, A. Otsuka, Y. Yoshida, R. N. Lyubovskaya, *J. Am. Chem. Soc.* **2003**, *125*, 10074–10083; d) D. V. Konarev, S. S. Khasanov, A. Otsuka, G. Saito, *J. Am. Chem. Soc.* **2002**, *124*, 8520–8521.
[13] a) M. Schulz-Dobrick, M. Panthöfer, M. Jansen, *Eur. J. Inorg. Chem.* **2005**, 4064–4069; b) A. L. Balch, *Chem. Commun.* **2002**, 1352–1353; c) D. V. Konarev, *J. Solid State Chem.* **2002**, *168*, 474–485; d) R. N. Lyubovskaya, *CrystEngComm* **2002**, 618–622; e) I. Ikemoto, *Inorg. Chim. Acta* **2001**, *317*, 81–90.
[14] a) R. C. Haddon, *Acc. Chem. Res.* **1992**, *25*, 127–133; b) N. Koga, K. Morokuma, *Chem. Phys. Lett.* **1992**, *196*, 191–196.
[15] J. Stinchcombe, A. Penicaud, P. Bhyrappa, P. D. W. Boyd, C. A. Reed, *J. Am. Chem. Soc.* **1993**, *115*, 5212–5217.

